THE JOURNAL OF PHYSICAL CHEMISTRY B

ARTICLE

pubs.acs.org/JPCB

Thermodynamic, Diffusional, and Structural Anomalies in Rigid-Body Water Models

Manish Agarwal, Mohammad Parvez Alam, and Charusita Chakravarty*

Department of Chemistry, Indian Institute of Technology-Delhi, New Delhi 110016, India

ABSTRACT: Structural, density, entropy, and diffusivity anomalies of the TIP4P/2005 model of water are mapped out over a wide range of densities and temperatures. The locus of temperatures of maximum density (TMD) for this model is very close to the experimental TMD locus for temperatures between 250 and 275 K. Four different water models (mTIP3P, TIP4P, TIP5P, and SPC/E) are compared with the TIP4P/2005 model in terms of their anomalous behavior. For all the water models, the density regimes for anomalous behavior are bounded by a low-density limit at around 0.85−0.90 g cm^{-3} and a high-density limit at about 1.10−1.15 g cm^{-3}. The onset temperatures of the density anomaly in the various models show a much greater variation, ranging from 202 K for mTIP3P to 289 K for TIP5P. The order maps for the various water models are qualitatively very similar with the structurally anomalous regions almost superimposable in the $q_{tet}-\tau$ plane. Comparison of the phase diagrams of water models with the region of liquid-state anomalies shows that the crystalline phases are much more sensitive to the choice of water models than the liquid state anomalies; for example, SPC/E and TIP4P/2005 show qualitatively similar liquid state anomalies but very different phase diagrams. The anomalies in the liquid in all the models occur at much lower pressures than those at which the melting line changes from negative to positive slope. The results in this study demonstrate several aspects of structure−entropy−diffusivity relationships of water models that can be compared with experiment and used to develop better atomistic and coarse-grained models for water.

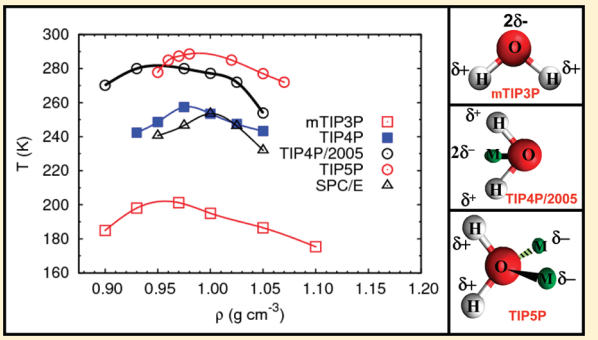

1. INTRODUCTION

The importance of water in chemical and biological processes implies that reliable potential models for water that describe its role as a solvent are very necessary. Developing computationally efficient and accurate parametric potentials for water, however, poses a serious challenge given the complexity of interactions in water, with significant contributions from dispersion, many-body polarization, hydrogen bonding, and long-range electrostatic interactions.[1−4] The most widely used potentials for water are rigid-body, effective pair potentials, which include the SPC/E, ST2, and TIPnP models. All the models treat water as a rigid body and account for intermolecular interactions using a set of distributed Lennard-Jones and charge sites. While the differences between the water models are not large in terms of their ability to reproduce structural and thermodynamic properties under standard temperature and pressure conditions, the models differ significantly with regard to their ability to reproduce crucial features of the experimental phase diagram and liquid-state anomalies (see Table 2).[4−11] For example, the SPC/E model is known to qualitatively reproduce all anomalous properties of water but typically at temperatures that are 30−40 K lower than the experimental value of 279 K. The TIP3P model is widely used in biomolecular simulations, but the onset temperature for anomalous behavior is 170−200 K.[3,7,9] The recently proposed TIP4P/2005 is currently the most accurate rigid-body model in terms of its ability to reproduce the bulk phase diagram and the equation of state of liquid water at ambient pressure.

Since the anomalous properties of bulk water are connected with its solvation properties,[12−16] an understanding of the relationship between liquid state structure, thermodynamics, and transport properties is essential for designing better water potentials at an atomistic as well as coarse-grained level.[17,18] An important development in this respect has been the analysis of structure−entropy−diffusivity relationships in liquids in terms of the excess entropy, S_e, defined as the difference between the total thermodynamic entropy (S) and the corresponding ideal gas entropy (S_{id}) at the same temperature and density. A necessary, though not sufficient, condition for a fluid to show water-like thermodynamic and transport anomalies is the existence of an excess entropy anomaly, corresponding to a rise in excess entropy, S_e, on isothermal compression ($(\partial S_e/\partial \rho)_T > 0$).[7,19−30] Liquids with water-like anomalies display distinct forms of local order or length scales in the low- and high-density regimes; competition between the two types of local order results in a rise in excess entropy at intermediate densities. Most liquids, including anomalous ones, obey semiquantitative excess entropy scaling relationships for transport properties of the form $X^* = A \exp(\alpha S_e)$ where X^* are reduced transport coefficients and A and α are scaling parameters that are very similar for systems with

Received: November 9, 2010
Revised: April 6, 2011
Published: May 10, 2011

conformal potentials.[31−34] Consequently, the existence of an excess entropy anomaly is reflected in mobility anomalies.

A rigorous connection between structural correlations and thermodynamics of fluids can be made using multiparticle correlation expansions of the entropy which allows one to write the excess entropy as a sum of pair and higher-order correlation terms[35−38]

$$S_e = S_2 + S_3 + S_4 + \ldots \quad (1)$$

For a binary system consisting of a total number of N structureless particles enclosed in a volume V at temperature T, the pair correlation entropy (S_2) will be given by[37]

$$S_2/Nk_B = -2\pi\rho \sum_{\alpha,\beta} x_\alpha x_\beta \int_0^\infty \{g_{\alpha\beta}(r)\ln g_{\alpha\beta}(r) - [g_{\alpha\beta}(r) - 1]\} r^2 dr \quad (2)$$

where $g_{\alpha\beta}(r)$ is the pair correlation function between spherically symmetric particles of type α and type β and x_α is the mole fraction of particles of type α. S_2 is typically the dominant contribution and accounts for 80−90% of S_e for simple liquids. In the case of a molecular fluid like water, the importance of three-body correlations associated with bond angle constraints in water reduces the quantitative accuracy of S_2 as a structural estimator for S_e. Nonetheless, we have found S_2 constructed from O−O, O−H, and H−H radial distribution functions to be qualitatively similar to S_e in terms of locating regimes of anomalous liquid state behavior as well as diffusivity scaling.[7,29]

While aspects of the excess entropy picture of water-like anomalies have been studied for various models,[7,25,28,29,39] there is no consolidated study of a single water model covering the relationships between structural, entropy, density, and diffusivity anomalies that can serve as a basis for comparison of the behavior of different water models. In this paper, we map out the anomalous regime in liquid-state behavior of the TIP4P/2005 model and relate it to the phase diagram. We then compare several widely used water models, especially with regard to structural order and pair entropy anomaly, since the structural basis for anomalous behavior in tetrahedral liquids can be formulated in terms of the competition between orientational and pair correlation order metrics and has proved to be a very influential idea in our understanding of anomalous fluids.[5] Our results suggest that comparison of such structural order metrics and entropy measures derived from simulations with structural data derived from neutron scattering experiments would be worthwhile.[40,41] We also discuss the implications for developing better potential models, coarse-graining schemes, and quantum simulation algorithms.

The paper is organized as follows. Section 2 summarizes the computational methods for molecular dynamics simulations of the five models of water studied here, namely, SPC/E, mTIP3P, TIP4P, TIP5P, and TIP4P/2005. Section 3 discusses our results for the TIP4P/2005 model. Section 4 provides a comparison of crucial aspects of various water models. Section 5 summarizes our conclusions.

2. COMPUTATIONAL DETAILS

All the five water models studied here correspond to rigid-body, effective pair potentials. The parametric form of the interaction between two water molecules a and b is given by

$$U_{ab} = \sum_i \sum_j \frac{q_i q_j}{r_{ij}} + 4\varepsilon\left(\frac{\sigma^{12}}{r_{OO}^{12}} - \frac{\sigma^6}{r_{OO}^6}\right) \quad (3)$$

where i and j index partial charges located on molecules a and b, respectively, and r_{OO} refers to the distance between the oxygen atoms of the two monomers.[42,43] All the rigid-body, effective pair potentials for water assume that the molecule can be represented by a single Lennard-Jones site located on oxygen atoms and model the charge distribution by a set of distributed charges with a fixed geometry. The parameters for all the rigid-body water models studied in this work are conveniently summarized in Table 1. For all water models other than the mTIP3P, the parameters are the same as those given in ref 11. The mTIP3P model corresponds to a modified version of TIP3P widely used in biomolecular simulations in conjunction with the CHARMM force field.[44]

Table 1. Parameters for Rigid-Body Water Models[a]

parameters	SPC/E	TIP3P	mTIP3P	TIP4P	TIP4P/2005	TIP5P
ε_{OO}(kcal/mol)	0.155	0.152	0.152	0.155	0.1851	0.160
σ_{OO} (Å)	3.1656	3.1506	3.1506	3.1540	3.1589	3.120
ε_{HH} (kcal/mol)	-	-	0.0460	-	-	-
σ_{HH} (Å)	-	-	0.4000	-	-	-
ε_{OH} (kcal/mol)	-	-	0.0836	-	-	-
σ_{OH} (Å)	-	-	1.7755	-	-	-
r_{OH} (Å)	1.000	0.9572	0.9572	0.9572	0.9572	0.9572
r_{OM} (Å)	-	-	-	0.15	0.1546	-
r_{OL} (Å)	-	-	-	-	-	0.70
∠HOH (deg)	109.47	104.52	104.52	104.52	104.52	104.52
q_O (e)	−0.8472	−0.8340	−0.8340	-	-	-
q_H (e)	0.4238	0.417	0.417	0.52	0.5564	0.241
q_M (e)	-	-	-	−1.04	−1.1128	-
q_L (e)	-	-	-	-	-	−0.241

[a] Parameters for the mTIP3P model are from ref 44, while parameters for all the other models are taken from ref 11.

Molecular dynamics simulations of water models were performed in the NVT ensemble using the Verlet algorithm as implemented in the DL_POLY package[45] using 256 molecules in a cubic simulation box with 1 fs time step in the Verlet scheme. State points for water models covered a density range from 0.85 to 1.4 g cm^{-3}. Temperature ranges and other computational details are given in Table 3. Various structural data from the literature was reproduced for each model to test the quality of simulations. We note that the data presented here for SPC/E, mTIP3P, and TIP5P models are from much longer simulations than those presented in ref 7. Diffusivities were computed using the Einstein relation; the trajectory was written to disk every 500 fs, and the mean square displacements were computed over 1 ns sections of the trajectories. Errors in the diffusivities were estimated by averaging over these 4−5 splits and were of the size of symbols at most statepoints.

The locus of minima in the $P-T$ curves was prepared with cubic spline smoothed data. More simulations were done along intermediate densities and temperatures, as required to improve statistics on the final locus.

The excess entropy calculations were done using thermodynamic integration, with the reference state as a gas of rigid triatomics at 1000 K, 0.01 g cm^{-3}, as described in ref 46. As a check on our excess entropy calculations, we note that our values for SPC/E differ from those computed by Chopra et al. in ref 30

Table 2. Thermodynamic Data for the Melting Transition and Density Anomaly of Water[a]

	melting point		$TMD_{1\ atm}$		TMD_{MAX}	
model	T_l (K)	ρ_l (g cm^{-3})	T_{1atm}^{TMD} (K)	ρ_{1atm}^{TMD} (g cm^{-3})	T^m (K)	ρ^m (g cm^{-3})
mTIP3P	146	1.017	182	1.038	202	0.956
SPC/E	215	1.007	241	1.012	253	1.0
TIP4P	232	1.002	253	1.008	257	0.98
TIP4P/2005	252	0.993	280	0.999	282	0.95
TIP5P	274	0.987	285	0.989	289	0.99
H_2O	273.15	0.99983	277.13	0.99997	-	-

[a] The first two columns provide the melting point temperature and liquid density at 1 atm pressure.[9] The temperature and maximum density at 1 atm are provided in the next two columns.[9] The last two columns contain data from this study on the maximum temperature and associated density along the TMD locus.

Table 3. Computational Details of MD Simulation for Different Water Models[a]

parameters	SPC/E	mTIP3P	TIP4P	TIP5P	TIP4P/2005
rigid constraints	SHAKE	SHAKE	quaternion	quaternion	quaternion
τ_B (ps)	1	20	200	20	20
T (K)	220−300	170−300	230−320	250−320	240−310

[a] The number of water molecules used in all simulations was 256. An MD time step of 1 fs was used for all five systems. The time constant for the Berendsen thermostat is denoted by τ_B. Equilibration and production run lengths are 4−6 ns and 4 ns, respectively. Temperature ranges are given in the last row. Densities are in the range of 0.80−1.40 g cm^{-3}. Variations in the dynamic and static properties due to change in thermostat relaxation time from 20 to 200 ps are less than the simulation errors.

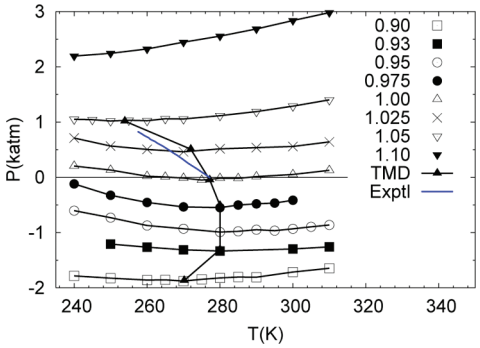

Figure 1. Pressure−temperature ($P(T)$) curves along various isochores and the locus of temperatures of maximum density (TMD) for the TIP4P/2005 model from NVT ensemble simulations reported here. The experimental TMD line is shown using blue-filled diamonds, taken from ref 48.

by 0.15−0.20 Nk_B. The pair entropy was estimated using eq 2. It should be noted that the thermodynamic excess entropy calculated via thermodynamic integration uses as a reference state an ideal gas of rigid rotors, denoted by S_{tri}. On the other hand, the pair correlation entropy assumes the system to be a mixture of two ideal gases, similar to that in the case of ionic melts,[7] denoted by S_{bin}. There will be a constant entropy difference of $S_{bin}(T_r,V_r) - S_{tri}(T_r,V_r)$, corresponding to removal of certain degrees of freedom associated with imposition of rigid-body constraints.

3. LIQUID-STATE ANOMALIES OF THE TIP4P/2005 MODEL

3.1. Density Anomaly. The region of thermodynamic anomaly in the phase diagram, within which density (ρ) increases on isobaric heating, is bounded by the locus of temperatures of maximum density (TMD) for which $(\partial\rho/\partial T)_P = 0$. For isochores passing through this anomalous regime, the TMD locus corresponds to the extrema in the $P(T)$ curves, i.e., state points for which $(\partial P/\partial T)_V = 0$. The state point corresponding to the maximum in temperature along the TMD locus is denoted by (ρ^m, T^m) and represents the maximum temperature at which the density anomaly can be observed. Figure 1 shows the $P(T)$ isochores and the locus of TMD points for the TIP4P/2005 model. The TIP4P/2005 model closely parallels the TMD line between 250 and 280 K, though the experimental data cannot be followed at negative pressures and therefore do not show the parabolic behavior seen in the simulations. It should be noted that the density anomaly, in conjunction with the negative slope of the TMD locus ($(dP/dT)_{TMD} < 0$), can be shown on the basis of purely thermodynamic arguments to lead to water-like anomalous behavior of the compressibility (κ) and the isobaric heat capacity (C_p), as discussed in detail elsewhere.[4,47]

3.2. Excess and Pair Entropy Anomalies. Figure 2(a) shows the behavior of the thermodynamic excess entropy as a function of density for various isotherms of the TIP4P/2005 model. Using simple thermodynamic arguments, one can show that state points lying on the TMD locus must correspond to those for which $(\partial P/\partial T)_V = (\partial S/\partial V)_T = 0$. Since $S = S_{id} + S_e$ and S_{id} is a monotonic function of density, the existence of a density anomaly must imply nonmonotonic behavior of the excess entropy with density. The excess entropy anomaly is defined as a temperature−density regime within which $(\partial S_e/\partial\rho)_T > 0$. Figure 2(a) shows that at 240 K $(\partial S_e/\partial\rho)_T > 0$ for densities lying between 0.85 and 1.1 g cm^{-3}. With increasing temperature, the strength as well as the density range of the excess entropy anomaly decrease, and by 300 K, only a plateau in the $S_e(\rho)$ curve remains. At low temperatures, densities below 0.85 g cm^{-3} could not be observed because they were found to be thermodynamically unstable with $\kappa < 0$. Within the accessible density range, for most of the isotherms, a maximum in $S_e(\rho)$ can be located which marks the high-density boundary of the region of excess entropy anomaly in the $\rho-T$ plane, while the minimum in $S_e(\rho)$ can be located only for the 290 and 300 K isotherms.

dx.doi.org/10.1021/jp110695t |J. Phys. Chem. B 2011, 115, 6935–6945

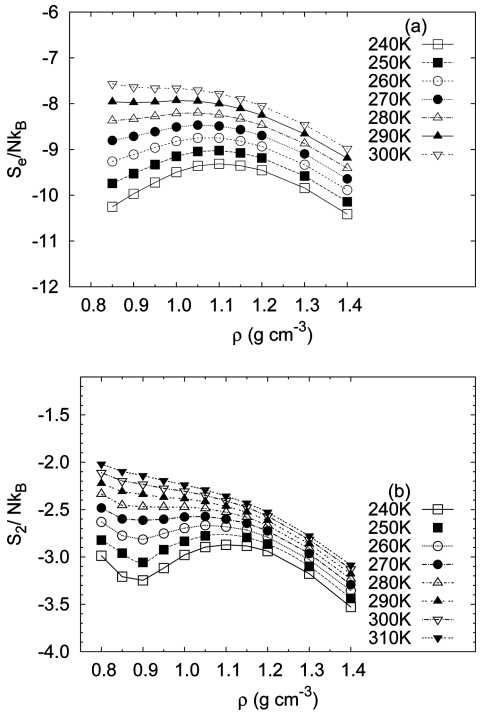

Figure 2. Isothermal variation with density of (a) thermodynamic excess entropy and (b) pair correlation entropy for the TIP4P/2005 model.

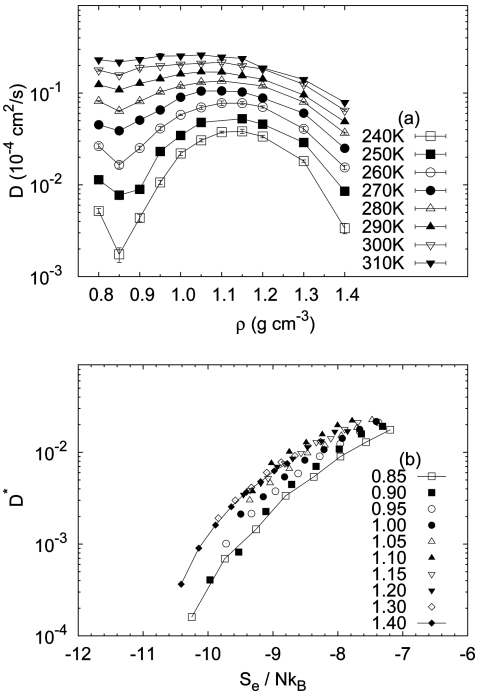

Figure 3. (a) Isothermal variation of diffusivity with temperature and (b) correlation of dimensionless diffusivities ($D^* = D(\rho_n^{1/3}/(k_BT/m)^{1/2})$) with excess entropy for the TIP4P/2005 water model.

Previous work suggests that the pair correlation entropy (S_2), constructed from O−O, O−H, and H−H RDFs, is a reasonable qualitative estimator for S_e.[7,29] Figure 2(b) shows S_2 as a function of density for various isotherms to locate the pair correlation entropy anomaly (PCEA) for the TIP4P/2005 model. Like the excess entropy anomaly, the pair correlation entropy anomaly is pronounced at 240 K and reduced to a plateau by 300 K. Unlike the $S_e(\rho)$ curves, the $S_2(\rho)$ curves show a minimum (at about 0.9 g cm^{-3}) as well as a maximum at 1.1 g cm^{-3}.

3.3. Diffusional Anomaly. The diffusional anomaly corresponds to a rise in diffusivity on isothermal compression ($(\partial D/\partial\rho)_T > 0$). Figure 3(a) shows the diffusional anomaly generated by the TIP4P/2005 model over several isotherms, including at 300 K. The relationship between transport anomalies and the excess entropy anomaly follows from the Rosenfeld-scaling rules. In the specific case of diffusivity, using macroscopic reduction parameters based on elementary kinetic theory, one can define reduced diffusivities as $D^* = D(\rho_n^{1/3}/(k_BT/m)^{1/2})$ where ρ_n is the number density.[32] Figure 3(b) shows that the logarithm of the reduced diffusivity is essentially a linear function of the excess entropy along an isochore. Small deviations from linearity are seen at low temperatures. Recent work suggests that these deviations arise from the onset of cooperative dynamics involving local caging effects.[49] Note that the exponential relationship between D^* and S_e implies that the diffusional anomaly is more pronounced than the excess entropy anomaly at 300 K. Recent experimental data show that viscosity of water, related to the diffusivity by the Stokes−Einstein relation, obeys the Rosenfeld-scaling relation for state points lying in the liquid and dense fluid regimes of the phase diagram.[50] The liquid−gas critical point of water occurs at 647 K and 0.218 GPa; the experimental data extends up to temperatures of 573 K and pressures of 60 GPa, covering a large part of the liquid phase region.[50] The simulation results for TIP4P/2005 are for relatively low temperatures up to 310 K, as a consequence of which the small isochore-dependent variations in Rosenfeld-scaling parameters are more obvious.

3.4. Structural Anomaly. Short-range tetrahedral order is one of the defining features of the structure of water which can be quantitatively measured using the local tetrahedral order parameter, q_{tet}. The q_{tet} value associated with an atom i is defined as

$$q_{tet} = 1 - \frac{3}{8}\sum_{j=1}^{3}\sum_{k=j+1}^{4}(\cos\psi_{jk} + 1/3)^2 \qquad (4)$$

where ψ_{jk} is the angle between the bond vectors $\mathbf{r}_{ij}$ and $\mathbf{r}_{ik}$ where j and k label the four nearest neighbor atoms of the same type.[5,51] Figure 4(a) shows the characteristic behavior of isothermal $q_{tet}(\rho)$ plots of tetrahedral liquids with a maximum at low density, close to the ice density in the case of water models. The pair correlation or translational order parameter, τ, measures the extent of pair correlations present between tetrahedral centers (e.g., O in H_2O) and is defined as

$$\tau = (1/\xi_c)\int_0^{\xi_c}|g(\xi) - 1|d\xi \qquad (5)$$

where $\xi = r\rho^{1/3}$; r is the pair separation; $g(\xi)$ is the pair correlation function; and ξ_c is a suitably chosen cutoff distance.[52,53] Figure 4(b) shows the isothermal $\tau(\rho)$ plots with both maxima and minima. The maxima in $\tau(\rho)$ and q_{tet} occur at essentially the same density.

An order map shows the location of state points on a two-dimensional plane with the axes corresponding to orientational and translational order. The structurally anomalous region was originally defined by Errington and Debenedetti as the set of state points in the density−temperature (ρT)-plane for which q_{tet} and τ are strongly correlated, irrespective of density or temperature. The structurally anomalous region was shown to be closely

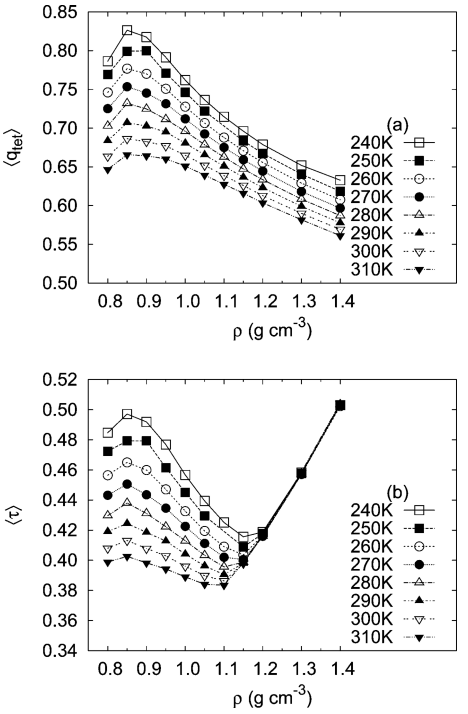

Figure 4. Constant temperature variation with density of (a) maxima in the local tetrahedral order parameter, q_{tet}, and (b) minima in the translational order, τ.

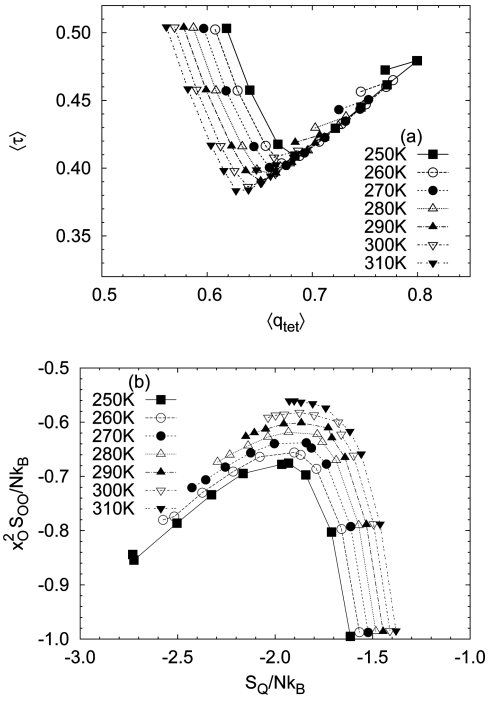

Figure 5. Correlation of (a) q_{tet} with τ and (b) S_Q with $x_O^2 S_{OO}$ for the TIP4P/2005 water model.

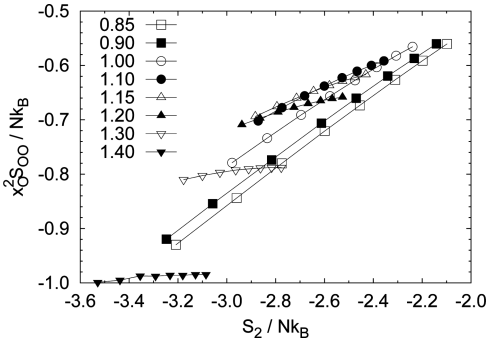

Figure 6. Correlation of total pair entropy, S_2, and the S_{OO} contribution.

associated with the region of diffusional anomaly, which in turn encloses the region of density anomaly. Figure 5(a) shows the order map of the TIP4P/2005 water model which strongly resembles order maps for SPC/E water though the anomalous regime is shifted to higher temperatures. We note that an alternative definition of the structurally anomalous regime can be provided by considering the locus of maxima and minima in $\tau(\rho)$. This definition is typically more convenient for tetrahedral ionic melts or core-softened fluids where the correlation between the two order metrics is not as strong.[18,28,54,55]

It is evident from the definitions in eqs 5 and 2 that the translational order metric, τ, and the contribution to the entropy from the oxygen−oxygen pair correlations, S_{OO}, both measure short-range order due to the same subset of pair correlations. This suggests the interesting possibility of converting order metrics into entropic measures. The magnitude of a given structural measure for entropy in comparison to the thermodynamic excess entropy allows one to gauge the importance of a given order metric in determining thermodynamic and transport behavior. From eq 2, the quantity $x_O^2 S_{OO}$ can be treated as the entropic analogue of τ, while S_2 can be treated as a measure of ordering due to all types of pair correlations. Entropic measures of orientational order have been discussed previously in the literature, though there has been no comparison of these different measures,[56−59] and given the coupling of orientational and translational order, a rigorous separation of the two contributions to the entropy is not possible. Here we follow the approach of Kumar and co-workers and define "tetrahedral entropy" at a state point (T,ρ) as[59]

$$S_Q(\rho,T) = \frac{3}{2}k_B\int_{Q_{min}}^{Q_{max}} \ln(1-Q)P(Q,T)\mathrm{d}Q \qquad (6)$$

where Q is the tetrahedral order parameter, q_{tet}. All distributions $P(Q)$ are normalized so that $\int_Q P(Q)\mathrm{d}Q = 1$. We note that S_Q is measured relative to S_0 where $S_0 = k_B[\ln \Omega_0 + 3/2 \ln(8/3)]$.

Figure 5(b) shows an "entropic" map, analogous to the order map, showing the correlation between tetrahedral and pair correlation entropies along isotherms. The conversion of order metrics to entropic measures separates the isochores belonging to the structurally anomalous regime, in a similar fashion to that seen using alternate measures of orientational order.[56] The inversion of the order and entropic maps is due to the anticorrelation between q_{tet} and S_Q. Note that the S_{OO} contribution is relatively small compared to the magnitude of S_2 (see Figure 6), as may be expected on the basis of the mole fractions. The magnitude of S_Q for the low density, low temperature isochores is, however, comparable with that of S_2. In this structurally anomalous regime, S_e and S_2 are therefore strongly correlated with tetrahedral order.

dx.doi.org/10.1021/jp110695t |J. Phys. Chem. B 2011, 115, 6935–6945

4. COMPARISON OF WATER MODELS

4.1. Density Anomaly. The density anomaly for various water models along the 1 atm pressure has been compared previously.[9] In this paper, our additional simulations have been directed at mapping out the TMD locus in the density−temperature plane for the various models, shown in Figure 7. The important features of the density anomaly are summarized in Table 2. The melting points, T_l, the TMD along the 1 atm isobar (ρ_{1atm}^{TMD}, T_{1atm}^{TMD}), and maxima of the TMD curves (ρ^m, T^m) for various models are given in Table 2. It is evident that T_l, T_{1atm}^{TMD}, and T^m follow the same trend for all models. The corresponding ρ_l as well as ρ_{1atm}^{TMD} are inversely correlated and decrease systematically. However, the ρ^m shows no specific trend. This might be attributed to the fact that the maxima of the loci of TMDs fall in the negative pressure regime for all five models. Although numerically the density range for all water models is very similar, the high accuracy in density measurements—both experimentally and in simulations—makes the variation of ≈10% quite significant.

4.2. Structural Anomaly. The structural anomaly in water-like fluids, defined as a regime of strong correlation between tetrahedral and translational order, has been discussed in Section 3.4 for the TIP4P/2005 water model. In Figure 8, we compare the order maps for three other TIPnP models and SPC/E water. The order map for SPC/E water is available in the literature but is shown here for convenience.[5] It may be noted that the SPC/E model does not have the same rigid-body geometry for the water molecule as the TIPnP family of models. All the water models give rise to very similar order maps. This is highlighted in Figure 9 which compares the structurally anomalous regime of the different water models in the $q_{tet}-\tau$ plane. The density range for the structural anomaly in all the models is the 0.85−1.30 g cm^{-3} regime. However, the temperature range associated with anomalous structural behavior varies over 150−200%. For example, the mTIP3P model shows a structurally anomalous regime below 240 K. In comparison, the TIP5P model has anomalous high temperatures of up to 320 K. This is consistent with earlier studies using the pair entropy as a diagnostic for anomalous regimes of water models.[7,28]

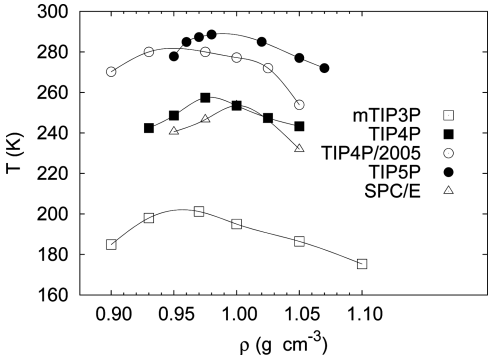

Figure 7. Comparison of the region of density anomaly in the density−temperature plane for different water models.

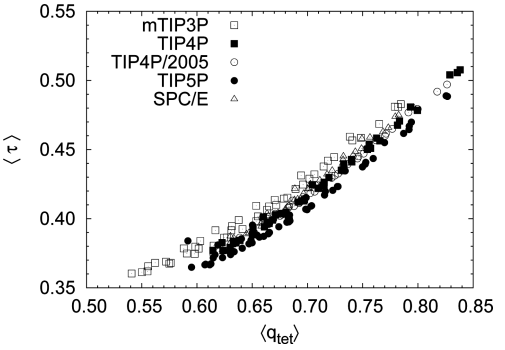

Figure 9. Structurally anomalous state points in the $q_{tet}-\tau$ order maps of various water models.

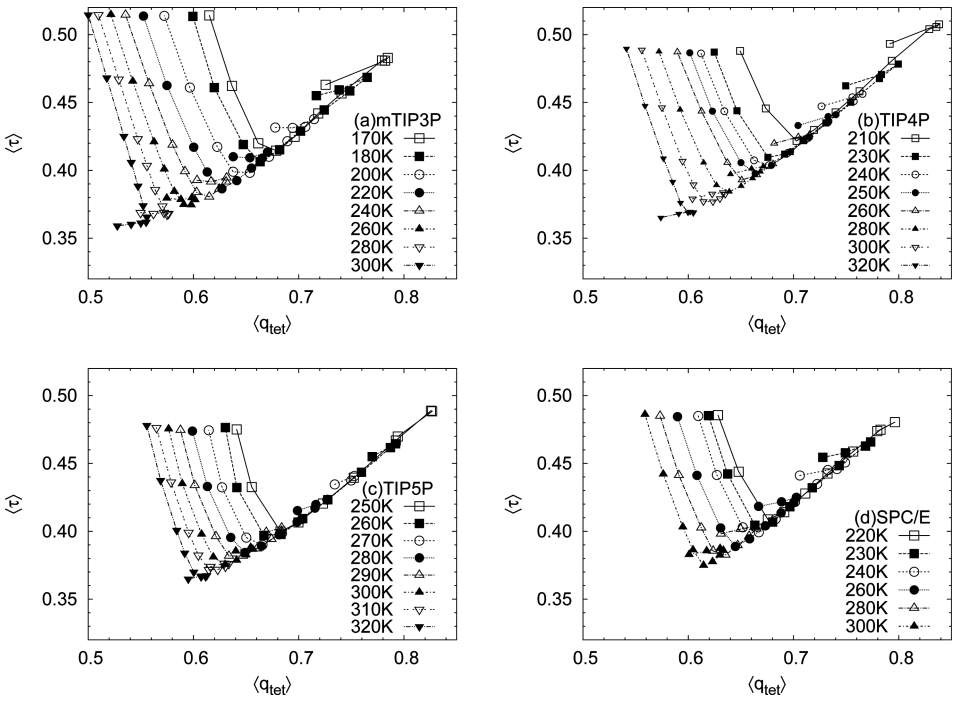

Figure 8. Order maps for various water models: (a) mTIP3P, (b) TIP4P, (c) TIP5P, and (d) SPC/E.

dx.doi.org/10.1021/jp110695t |J. Phys. Chem. B 2011, 115, 6935–6945

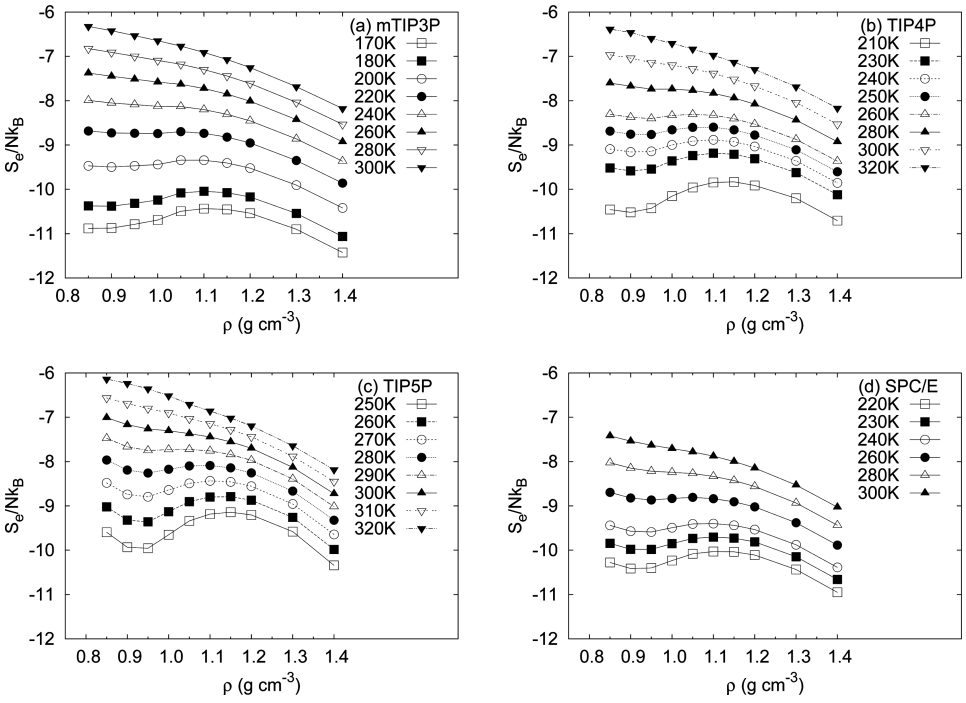

Figure 10. Excess entropy anomaly: variation of excess entropy, S_e, with density, along various isotherms: (a) mTIP3P, (b) TIP4P, (c) TIP5P, and (d) SPC/E.

In an earlier study, we have compared the order map of SPC/E water with three tetrahedral ionic melts (BeF_2, SiO_2, and GeO_2).[28] The tetrahedral ionic melts have a much weaker degree of correlation between the two order metrics, even within the anomalous regime, and access somewhat smaller values of q_{tet}. The water models appear to mark the boundary of the accessible region in the high q_{tet}−low τ plane for tetrahedral liquids.

The possibility of testing the presence of a structural anomaly in water using experimental data has so far not been considered. The translational order metric can be estimated from PDFs obtained from scattering measurements. Empirical potential structure refinement (EPSR) methods also generate configurations that are consistent with experimental structure factors.[41] It would be interesting to compute the tetrahedral order distributions and order maps from EPSR data with simulations based on different water models.

4.3. Excess and Pair Entropy Anomalies. Figure 10 shows the excess entropy anomaly for all the water models studied here, in addition to the results for TIP4P/2005 given in Figure 2. The range of excess entropy values and the density regime for anomalous behavior are very similar for all the models. As expected on the basis of density and structural anomalies, the temperature regime for anomalous behavior, however, shows significant variations for the different models. At the T^m of the TMD_{MAX} locus associated with each model, the positive slope of the $S_e(\rho)$ curve is similar for all the models. The most noticeable difference between the TIP4P/2005 model and all the other water models is the absence on a minimum in the $S_e(\rho)$ curves in the former. We also note that for all the water models S_e shows a $T^{-2/5}$ temperature scaling, consistent with the predictions for repulsive fluids made on the basis of density functional theory.[60]

Figure 11(a) compares the $S_e(\rho)$ curves for all the water models at 300 K. It can be seen that mTIP3P has the highest excess entropy, as well as clear monotonically decreasing trend with $((\partial S)/(\partial \rho))_T < 0$ which demonstrates the simple liquid behavior of the mTIP3P model under ambient conditions. All other models show either a weak excess entropy anomaly or a plateau indicating that the onset of the excess entropy anomaly is close to, but below, 300 K.

As emphasized elsewhere in this paper, the pair entropy is a very useful quantity for comparison between simulations and experiments. The isothermal behavior of the pair entropy for various water models has been already discussed for TIP4P/2005 in Section 3.4, and for other water models elsewhere in the literature.[7,29] The maxima and minima in $S_2(\rho)$ are close to the maxima in $q_{tet}(\rho)$ and minima in $\tau(\rho)$, respectively; therefore, it can provide an alternate definition of the structurally anomalous region. S_2 scales as $T^{-2/5}$ in the normal regime but shows deviations in the anomalous regimes. Here we restrict ourselves to a comparison of the $S_{OO}(\rho)$ and $S_2(\rho)$ curves at 300 K for the different water models in Figure 11. It is evident that S_{OO} coincides for the older (mTIP3P, SPC/E, and TIP4P) water models at 300 K close to 1 g cm^{-3}, presumably because they were designed to reproduce the O−O RDF at ambient conditions. Interestingly, the TIP5P and the TIP4P/2005 model, both of which describe the overall thermodynamic behavior and density anomalies relatively well, show significant differences from each other as well as the other water models. As expected, the mTIP3P water model shows simple liquid behavior at 300 K. It is also interesting to note the TIP4P/2005 and SPC/E water models show very similar $S_e(\rho)$ curves at 300 K.

From an experimental point of view, the accessible regime for obtaining atom−atom pair correlation functions in water by neutron scattering lies in the density range from 1.0 to 1.2 g cm^{-3} at temperatures above the melting temperature of water. The variations in S_2 and S_{OO} between the simulation models in the experimentally accessible density range are about 10−20% and will be accentuated at lower temperatures. The atom−atom pair

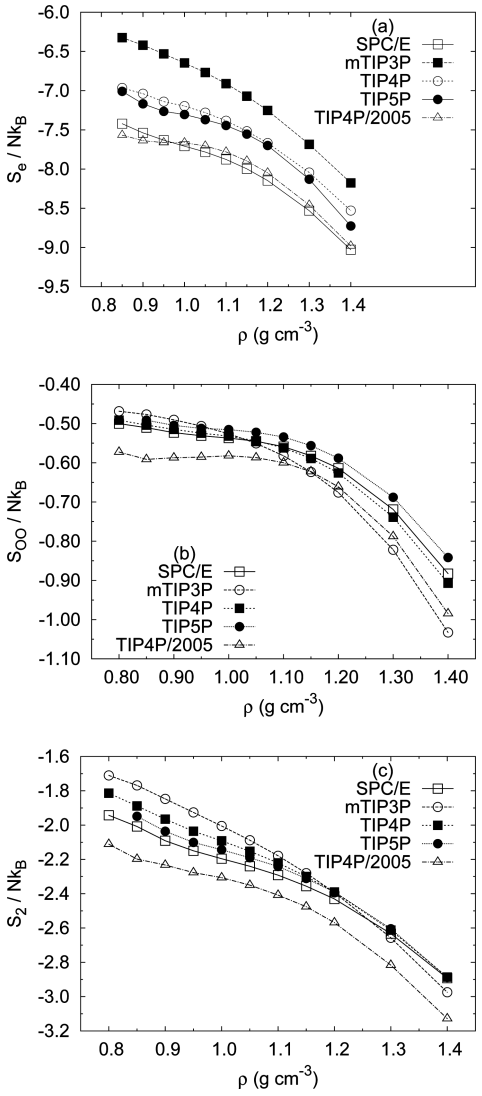

Figure 11. Variation with density of: (a) thermodynamic excess entropy, (b) oxygen−oxygen pair correlation entropy, S_{OO}, and (b) pair correlation entropy, S_2, along the 300 K isotherm for various water models.

correlation entropy may therefore be a useful quantity with significant short- and long-range contributions for benchmarking water potential models against experimentally available scattering data.

4.4. Diffusional Anomaly. The diffusional anomaly for all the five water models studied here shows a maximum diffusivity at the same density of 1.15 g cm^{-3} within simulation error. The minimum diffusivity, however, shifts in the sequence: TIP5P (0.925 g cm^{-3}) > mTIP3P ≈ SPC/E (0.9 g cm^{-3}) > TIP4P (0.875 g cm^{-3}) > TIP4P/2005 (0.85 g cm^{-3}). The temperature regimes showing anomalous diffusive behavior, however, are very different for the various water models and correlate with the anomalous regimes as predicted by the structural and pair entropy anomalies. In this paper, we compare only the diffusivities along the 300 K isotherm for all the five water models (see Figure 12). Among the models studied, only TIP4P/2005 shows a distinct diffusional anomaly for the 300 K isotherm. Rosenfeld scaling for all water models is qualitatively similar to that seen in TIP4P/2005.

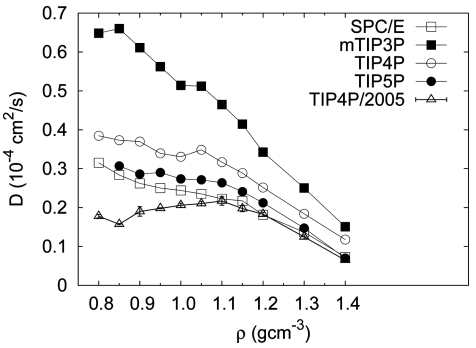

Figure 12. Diffusivity for various water models along the 300 K isotherm. Note the linear scale on the *y* axis. Errors at this temperature are of the symbol size or smaller.

4.5. Phase Diagram and Water-Like Anomalies. The excess entropy anomaly description of water-like anomalies is consistent with the relationships between the structure of the phase diagram and water-like anomalies developed earlier.[17,61−63] The energetically favorable local structures in condensed phases of water are tetrahedral at low densities and shift to a pair correlation-dominated order at high densities. In the crystalline phase with long-range translational symmetry requirements, the system can accommodate the necessary change in structure on compression only by undergoing a phase transition between two crystalline structures. In the case of a liquid, however, the change in local structure with compression needs not be discontinuous. However, competition between two types of order metrics at intermediate densities will result in a structurally frustrated regime at intermediate densities which will result in an excess entropy anomaly. Alternatively, the excess entropy anomaly can be viewed as an increase of excess entropy with increasing density due to the destruction of tetrahedral order at densities not yet high enough for this loss of ordering to be compensated by an increase in pair correlation ordering. To illustrate this, we juxtapose the nested regions of density, pair entropy, and structural anomalies on the phase diagram for TIP4P/2005 and SPC/E water models in Figure 13. The nested structure of anomalous regions was originally demonstrated by Errington and Debenedetti in the density−temperature plane and is referred to as the cascade of anomalies. Boundaries of the regions of anomalous regimes of structural, diffusivity, pair entropy, and density are shown for both the models in the temperature −pressure (TP) plane. Note that based on our state-point data we could create a smooth high-temperature boundary for only the density anomaly. For all the systems, this region of the density anomaly is enclosed within the other anomalous regimes. The structurally anomalous regime, defined in terms of q_{tet} and τ, is typically the widest. The low-density boundary of the region of pair entropy anomaly is very close to the locus of maxima in the tetrahedral order. The change in slope of the melting line for TIP4P/2005 water takes place around 300 MPa and 220 K, bordering the regions of stability of the ice Ih, ice III, and ice V phases. The liquid state anomalies in this model occur at slightly higher temperatures between 240 and 280 K but at pressures close to zero. As in the case of experiment, the low-pressure branch of the TMD locus actually falls in the negative pressure regime. The SPC/E model is unable to qualitatively reproduce the experimental phase diagram and shows a change in the sign of the slope of the melting line at about zero pressure and 220 K.

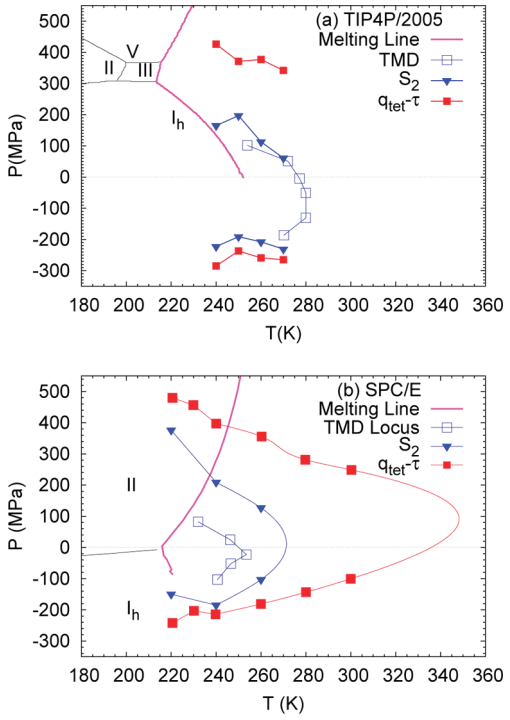

Figure 13. Phase diagram and cascade picture for the (a) TIP4P/2005 and (b) SPC/E water models. Data for the phase diagrams are taken from ref 11.

The anomalies occur slightly above this temperature and at zero pressure. In all the tetrahedral ionic melts and water models that we have studied so far,[28] the maximum temperature along the TMD locus tends to be at very low pressure compared to the pressures at which there is a change in slope of the melting line. As a consequence, part of the TMD locus lies in the negative pressure region. This also seems to be the case based on experimental data for water and silica.[64] Thus, it would appear that the readjustment of local structures to give rise to the excess entropy and related anomalies is initiated at very low pressures in liquids; in contrast, high pressures are required to effect a change in local structure in the solid phase.

5. DISCUSSION AND CONCLUSIONS

Structural, density, entropy, and diffusivity liquid-state anomalies of the TIP4P/2005 water model are mapped out over a wide range of densities and temperatures. The locus of temperatures of maximum density (TMD) for this model is very close to the experimental TMD locus for temperatures between 250 and 275 K. The excess and pair correlation entropy anomalies, known to be necessary conditions for the existence of water-like anomalies, are mapped out for this model. Rosenfeld-scaling is shown to be approximately valid for the TIP4P/2005 model as a result of which the excess entropy anomaly is associated with a diffusional anomaly. The structural anomaly is mapped out by locating the state points which show strong correlation between tetrahedral (q_{tet}) and translational (τ) order. Conversion of these order metrics to their equivalent entropy measures is shown to provide some insight into the importance of different order metrics in controlling the overall degree of disorder at different state points.

Four different water models (mTIP3P, TIP4P, TIP5P, SPC/E) are compared with the TIP4P/2005 model in terms of their anomalous behavior. For all the water models, the density regimes for anomalous behavior are bounded by a low-density limit at around 0.85−0.90 g cm^{-3} and a high-density limit at about 1.10−1.15 g cm^{-3}. The onset temperatures of the density in the various models show a much greater variation, with mTIP3P showing an anomalous regime at 170−210 K and TIP5P showing an onset temperature of 289 K. The TIP4P/2005 model provides the best agreement with experimental data.

The excess entropy anomaly for the various water models typically has an onset temperature slightly higher than the onset temperature for the density anomaly. The TIP4P/2005 model does not show any minimum in the isotherms for excess entropy as a function of temperature though all the models show a maximum at approximately 1.1 g cm^{-3}. The pair entropy anomaly is mapped out for various isotherms; in particular, the $S_2(\rho)$ curves for the different water models at 300 K show significant differences between water models and therefore may be useful for comparison with experiment. The order maps for the various water models are qualitatively very similar with the structurally anomalous regions almost superimposable in the $q_{tet}-\tau$ plane. Comparison of the phase diagrams of water models with the region of liquid-state anomalies shows that the crystalline phases are much more sensitive to the choice of water models than the liquid state anomalies; for example, SPC/E and TIP4P/2005 show qualitatively similar liquid state anomalies but very different phase diagrams. The anomalies in the liquid in all the models occur at much lower pressures than those at which the melting line changes from negative to positive slope. This reflects the ability of the disordered, liquid-state network to accommodate changes in local structure more readily than the solid phase.

The results in this study demonstrate several aspects of structure−entropy−diffusivity relationships of water models that can be compared with experiment and used to develop better atomistic models for water. The relationships between structural order and anomalous behavior can be compared with experiment using data from X-ray and neutron scattering, in conjunction with reverse Monte Carlo methods. This would be particularly useful since differences between the rigid-body potential models, particularly as indexed by the behavior of the pair correlation entropy, are significant in the experimentally accessible density and temperature regime. Interestingly, the TIP4P/2005 model is distinctly different from the other water models in the behavior of excess entropy, pair entropy, and diffusivity along the 300 K isotherm.

The two-order parameter model of water suggests that potentials which are more accurate for the crystalline phases would be more accurate for modeling anomalous behavior. The work of Vega, however, demonstrates that within the limitations of the rigid-body models separate parametrization of anomalous behavior and melting properties is required leading to the TIP4P/2005 and TIP4P/Ice models, respectively. We show that the anomalies in water-like liquids occur at pressures much lower than those at which the melting line changes the sign of slope, though the temperature regime for anomalous behavior is only slightly higher. Thus the interaction model must capture structural changes associated with increasing density in two very different pressure regimes. The fact that a single rigid-body model is unable to do both suggests that it may reflect some intrinsic limitations of the rigid-body parametric form for the potential or perhaps the need for finite temperature quantum simulations.

The comparison of classical and path integral simulations for liquid water clearly indicates the semiclassical character of the system with small but significant quantum effects.[65−67] It would therefore appear that much of the understanding of structure, entropy, and mobility relationships that has been developed for classical, rigid-body models could be readily extended using path integral simulations. The possibility of using quantum simulations with empirical structure refinement methods for analyzing neutron scattering data is also an interesting and unexplored possibility for which hybrid Monte Carlo algorithms would seem to be very suitable.[68]

We also note that there has been considerable interest in developing coarse-grained potential models for water that can be used in conjunction with models of solutes such as proteins and lipids. For example, isotropic models of water which reproduce the $g_{OO}(r)$ function have been constructed but have some problems with representability and transferability.[13,69−71] The structure−entropy−diffusivity relationships discussed in this work should be useful for developing coarse-graining strategies which are consistent with significant features of the behavior of bulk water.

AUTHOR INFORMATION

Corresponding Author

*Tel.: (+)91-11-2659-1510. Fax: (+)91-11-2686-2122. E-mail: charus@chemistry.iitd.ernet.in.

ACKNOWLEDGMENT

This work was financially supported by the Department of Science and Technology, New Delhi. M.A. would like to thank the Indian Institute of Technology-Delhi for award of a Senior Research Fellowship. C.C. would like to thank A. K. Soper for useful discussions. The authors would like to thank Divya Nayar for help in revising the manuscript.

REFERENCES

(1) Leach, A. R. *Molecular Modelling: Princliples and Applications*; Addison Wesley Longman: England, 1996.

(2) Dill, K. A.; Truskett, T. M.; Vlachy, V.; Hribar-Lee, B. Modeling water, the hydrophobic effect, and ion solvation. *Annu. Rev. Biophys. Biomol. Struct.* **2005**, *34*, 173–199.

(3) Jorgensen, W. L.; Chandrasekhar, J.; Madura, J. D.; Impey, R. W.; Klein, M. L. Comparison of simple potential functions for simulating liquid water. *J. Chem. Phys.* **1983**, *79*, 926.

(4) Debenedetti, P. G. Supercooled and glassy water. *J. Phys.: Condens. Matter* **2003**, *15*, R1669.

(5) Errington, J. R.; Debenedetti, P. G. Relationship between structural order and the anomalies of liquid water. *Nature* **2001**, *409*, 318.

(6) Scala, A.; Starr, F. W.; Nave, E. L.; Sciortino, F.; Stanley, H. E. Configurational entropy and diffusivity of supercooledwater. *Nature* **2000**, *406*, 166.

(7) Sharma, R.; Agarwal, M.; Chakravarty, C. Estimating entropy of liquids from atom-atom radial distribution functions: Silica, beryllium fluoride and water. *Mol. Phys.* **2008**, *106*, 1925.

(8) Vega, C.; Abascal, J. L. F. A general purpose model for the condensed phases of water: TIP4P/2005. *J. Chem. Phys.* **2005**, *123*, 234505.

(9) Vega, C.; Abascal, J. L. F. Relation between the melting temperature and the temperature of maximum density for the most common models of water. *J. Chem. Phys.* **2005**, *123*, 144504.

(10) Vega, C.; Sanz, E.; Abascal, J. L. F.; Noya, E. G. Determination of phase diagrams via computer simulation: methodology and applications to water, electrolytes and proteins. *J. Phys.: Condens. Mater.* **2008**, *20*, 153101.

(11) Vega, C.; Abascal, J. L. F.; Conde, M. M.; Aragones, J. L. What ice can teach us about water interactions: a critical comparison of the performance of different water models. *Faraday Discuss.* **2009**, *141*, 251.

(12) Paschek, D. Temperature dependence of the hydrophobic hydration and interaction of simple solutes: An examination of five popular water models. *J. Chem. Phys.* **2004**, *20*, 6674.

(13) Lynden-Bell, R. M.; Head-Gordon, T. Solvation in modified water models: towards understanding hydrophobic effects. *Mol. Phys.* **2006**, *104*, 3593.

(14) Nutt, D. R.; Smith, J. C. Molecular dynamics simulations of proteins: Can the explicit water model be varied? *J. Chem. Theory Comput.* **2007**, *3*, 1550.

(15) Chatterjee, S.; Debenedetti, P. G.; Stillinger, F. H.; Lynden-Bell, R. M. A computational investigation of thermodynamics, structure, dynamics and solvation behavior in modified water models. *J. Chem. Phys.* **2008**, *128*, 124511.

(16) Agarwal, M.; Kushwaha, H. R.; Chakravarty, C. Local order, energy, and mobility of water molecules in thehydration shell of small peptides. *J. Phys. Chem. B* **2010**, *114*, 651.

(17) Molinero, V.; Moore, E. B. Water modeled as an intermediate element between carbon and silicon. *J. Phys. Chem. B* **2009**, *113*, 4008.

(18) Chaimovich, A.; Shell, M. S. Anomalous waterlike behavior in spherically-symmetric water models optimized with the relative entropy. *Phys. Chem. Chem. Phys.* **2009**, *11*, 1901.

(19) Sharma, R.; Chakraborty, S. N.; Chakravarty, C. Entropy, diffusivity, and structural order in liquids with waterlike anomalies. *J. Chem. Phys.* **2006**, *125*, 204501.

(20) Agarwal, M.; Sharma, R.; Chakravarty, C. Ionic melts with waterlike anomalies: Thermodynamic properties of liquid BeF_2. *J. Chem. Phys.* **2007**, *127*, 164502.

(21) Agarwal, M.; Chakravarty, C. Waterlike structural and excess entropy anomalies in liquid beryllium fluoride. *J. Phys. Chem. B* **2007**, *111*, 13294.

(22) de Oliveira, A. B.; Franzese, G.; Netz, P. A.; Barbosa, M. C. Waterlike hierarchy of anomalies in a continuous spherical shouldered potential. *J. Chem. Phys.* **2008**, *128*, 064901.

(23) Mittal, J.; Errington, J. R.; Truskett, T. M. Relationship between thermodynamics and dynamics of supercooled liquids. *J. Chem. Phys.* **2006**, *125*, 076102.

(24) Mittal, J.; Errington, J. R.; Truskett, T. M. Erratum: "Relationship between thermodynamics and dynamics of supercooled liquids. *J. Chem. Phys.* **2010**, *132*, 169904; *J. Chem. Phys.* **2006**, *125*, 076102.

(25) Mittal, J.; Errington, J. R.; Truskett, T. M. Quantitative link between single-particle dynamics and static structure of supercooled liquids. *J. Phys. Chem. B* **2006**, *110*, 18147.

(26) Errington, J. R.; Truskett, T. M.; Mittal, J. Excess-entropy-based anomalies for a waterlike fluid. *J. Chem. Phys.* **2006**, *125*, 244502.

(27) Yan, Z.; Buldyrev, S. V.; Stanley, H. E. Relation of water anomalies to the excess entropy. *Phys. Rev. E* **2008**, *78*, 051201.

(28) Jabes, B. S.; Agarwal, M.; Chakravarty, C. Tetrahedral order, pair correlation entropy, and waterlike liquid state anomalies: Comparison of GeO_2 with BeF_2, SiO_2, and H_2O. *J. Chem. Phys.* **2010**, *132*, 234507.

(29) Agarwal, M.; Singh, M.; Sharma, R.; Alam, M. P.; Chakravarty, C. Relationship between structure, entropy and diffusivity inwater and water-like liquids. *J. Phys. Chem. B* **2010**, *114*, 6995.

(30) Chopra, R.; Truskett, T. M.; Errington, J. R. On the use of excess entropy scaling to describe the dynamic properties of water. *J. Phys. Chem. B* **2010**, *114*, 10558–10566.

(31) Rosenfeld, Y. Relation between transport coefficients and the internal entropy of simple systems. *Phys. Rev. A* **1977**, *15*, 2545.

(32) Rosenfeld, Y. A quasi-universal scaling law for atomic transport in simple fluids. *J. Phys.: Condens. Matter* **1999**, *11*, 5415.

(33) Dzugutov, M. A universal scaling law for atomic diffusion in condensed matter. *Nature (London)* **1996**, *381*, 137.
(34) Hoyt, J. J.; Asta, M.; Sadigh, B. Test of the universal scaling law for the diffusion coefficient in liquid metals. *Phys. Rev. Lett.* **2000**, *85*, 594.
(35) Green, H. S. *The Molecular Theory of Fluids*; North-Holland: Amsterdam, 1952.
(36) Baranyai, A.; Evans, D. J. Direct entropy calculation from computer simulation of liquids. *Phys. Rev. A* **1989**, *40*, 3817.
(37) Laird, B. B.; Haymet, A. D. J. Calculation of entropy from multiparticle correlation functions. *Phys. Rev. A* **1992**, *45*, 5680.
(38) Hernando, J. A. Thermodynamic potentials and distribution functions i. a general expression for the entropy. *Mol. Phys.* **1990**, *69*, 319.
(39) Krekelberg, W. P.; Mittal, J.; Ganesan, V.; Truskett, T. M. Structural anomalies of fluids: Origins in second and higher coordination shells. *Phys. Rev. E* **2008**, *77*, 041201.
(40) Soper, A. K. Probing the structure of water around biological molecules: concepts, constructs and consequences. *Phys. B* **2000**, *276*, 12.
(41) Soper, A. K. Tests of the empirical potential structure refinement method and a new method of application to neutron diffraction data on water. *Mol. Phys.* **2001**, *99*, 1503.
(42) Berendsen, H. J. C.; Grigera, J. R.; Straatsma, T. P. The missing term in effective pair potentials. *J. Phys. Chem.* **1987**, *91*, 6269.
(43) Mahoney, M. W.; Jorgensen, W. L. A five-site model for liquid water and the reproduction of the density anomaly by rigid, nonpolarizable potential functions. *J. Chem. Phys.* **2000**, *112*, 8910.
(44) Neria, E.; Fischer, S.; Karplus, M. Simulation of activation free energies in molecular systems. *J. Chem. Phys.* **1996**, *105*, 1902.
(45) Smith, W.; Yong, C. W.; Rodger, P. M. DL_POLY: Application to molecular simulation. *Mol. Simul.* **2002**, *28*, 385.
(46) Scala, A.; Starr, F. W.; Nave, E. L.; Stanley, H. E.; Sciortino, F. Free energy surface of supercooled water. *Phys. Rev. E* **2000**, *62*, 8016.
(47) Sastry, S.; Debenedetti, P. G.; Sciortino, F.; Stanley, H. E. Singularity-free interpretation of the thermodynamics of supercooled water. *Phys. Rev. E* **1996**, *53*, 6144.
(48) Fine, R. A.; Millero, F. J. The high pressure PVT properties of deuterium oxide. *J. Chem. Phys.* **1975**, *63*, 89.
(49) Agarwal, M.; Singh, M.; Jabes, B. S.; Chakravarty, C. Excess entropy scaling of transport properties in network-forming ionic melts (SiO_2 and BeF_2). *J. Chem. Phys.* **2011**, *134*, 014502.
(50) Abramson, E. H. Viscosity of water measured to pressures of 6 GPa and temperatures of 300 °C. *Phys. Rev. E* **2007**, *76*, 051203.
(51) Chau, P.-L.; Hardwick, A. J. A new order parameter for tetrahedral configurations. *Mol. Phys.* **1998**, *93*, 511.
(52) Torquato, S.; Truskett, T.; Debenedetti, P. Is random close packing of spheres well defined? *Phys. Rev. Lett.* **2000**, *84*, 2064.
(53) Truskett, T. M.; Torquato, S.; Debenedetti, P. G. Towards a quantification of disorder in materials: Distinguishing equilibrium and glassy sphere packings. *Phys. Rev. E* **2000**, *62*, 993.
(54) de Oliveira, A. B.; Netz, P. A.; Colla, T.; Barbosa, M. C. Structural anomalies for a three dimensional isotropic core-softened potential. *J. Chem. Phys.* **2006**, *125*, 124503.
(55) Pizio, O.; Dominguez, H.; Duda, Y.; Sokolowski, S. Microscopic structure and thermodynamics of a core-softened model fluid: Insights from grand canonical monte carlo simulations and integral equations theory. *J. Chem. Phys.* **2009**, *130*, 174504.
(56) Esposito, R.; Saija, F.; Marco Saitta, A.; Giaquinta, P. V. Entropy-based measure of structural order in water. *Phys. Rev. E* **2006**, *73* (4), 040502(R).
(57) Zielkiewicz, J. Structural properties of water: Comparison of the SPC, SPCE, TIP4P, and TIP5P models of water. *J. Chem. Phys.* **2005**, *123*, 104501.
(58) Zielkiewicz, J. Erratum: "Structural properties of water: Comparison of the SPC, SPCE, TIP4P, and TIP5P models of water. *J. Chem. Phys.* **2006**, *124* (10), 109901; *J. Chem. Phys.* **2005**, *123*, 104501.
(59) Kumar, P.; Buldyrev, S. V.; Stanley, H. E. A tetrahedral entropy for water. *Proc. Natl. Acad. Sci.* **2009**, *106*, 22130.
(60) Roseneld, Y.; Tarazona, P. Density functional theory and the asymptotic high density expansion of the free energy of classical solids and fluids. *Mol. Phys.* **1998**, *95*, 141.
(61) Tanaka, H. Thermodynamic anomaly and polyamorphism of water. *Euro. Phys. Lett.* **2000**, *50*, 340.
(62) Tanaka, H. Simple view of waterlike anomalies of atomic liquids with directional bonding. *Phys. Rev. B* **2002**, *66*, 064202.
(63) Molinero, V.; Sastry, S.; Angell, C. A. Tuning of tetrahedrality in a silicon potential yields a series of monatomic (metal-like) glass formers of very high fragility. *Phys. Rev. Lett.* **2006**, *97*, 075701.
(64) Brazhkin, V. V.; Lyapin, A. G. High-pressure phase transformations in liquids and amorphous solids. *J. Phys.: Condens. Matter* **2003**, *15*, 6059.
(65) Vega, C.; Conde, M. M.; McBride, C.; Abascal, J. L. F.; Noya, E. G.; Ramirez, R.; Sese, L. M. Heat capacity of water: A signature of nuclear quantum effects. *J. Chem. Phys.* **2010**, *132*, 046101.
(66) Noya, E. G.; Vega, C.; Sese, L. M.; Ramirez, R. Quantum effects on the maximum in density of water as described by the TIP4PQ/2005 model. *J. Chem. Phys.* **2009**, *131*, 124518.
(67) Habershon, S.; Markland, T. E.; Manolopoulos, D. E. Competing quantum effects in the dynamics of a flexible water model. *J. Chem. Phys.* **2009**, *131*, 024501.
(68) Chakravarty, C. Hybrid monte carlo implementation of the fourier path integral algorithm. *J. Chem. Phys.* **2005**, *123*, 024104.
(69) Louis, A. A. Beware of density dependent pair potentials. *J. Phys.: Condens. Matter* **2002**, *14*, 9187.
(70) Johnson, M. E.; Head-Gordon, T.; Louis, A. A. Represntability problems for coarsed-grained water potentials. *J. Chem. Phys.* **2007**, *126*, 144509.
(71) Head-Gordon, T.; Stillinger, F. H. An orientational perturbation theory for pure liquid water. *J. Chem. Phys.* **1993**, *98*, 3313.